



## INFLUENCE OF LENS ON MIGRATION OF DENSE NON-AQUEOUS PHASE LIQUID IN SATURATED ZONE

Prof. Dr. Waleed M. S. Kassim

Dr. Ayad A. H. Al-Dulaimi

Tamara Kawther Hussein

Environmental Engineering Department, College of Engineering, University of Baghdad

### ABSTRACT

This study concerns the control of movement of Dense Non-Aqueous Phase Liquid (DNAPL) in saturated zone in the presence of relatively low permeability lens. A two-dimensional, finite-difference numerical model for the simultaneous movement of the DNAPL and water through the saturated zone of the soil is developed. The system is, actually, a three fluid phase system (water, DNAPL and air) but in the derivation of the model, air was treated as an immobile phase at constant atmospheric pressure. The flow equations for Dense Non-Aqueous Phase Liquid and water are cast in terms of the wetting and non-wetting fluid pressure heads respectively. The finite-difference equations are solved fully implicitly using Newton-Raphson iteration scheme with a Taylor series expansion to treat the nonlinearity. The present numerical results are compared with results of Kueper and Frind (1991b). The results of all tests showed that the presence of lens controls the vertical movement of Dense Non-Aqueous Phase Liquid (DNAPL) in heterogeneous porous medium.

### تأثير وجود حاجز على حركة السوائل العضوية الاثقل من الماء في الطبقة مشبعة من التربة

#### الخلاصة

تتعلق هذه الدراسة بالسيطرة على حركة السوائل العضوية الاثقل من الماء، المسماة (Dense Non-Aqueous Phase Liquids (DNAPL<sub>s</sub>)) في الطبقة المشبعة من التربة بواسطة استخدام حاجز قليل النفاذية نسبياً. تم تطوير نموذج عددي ذو بعدين واستخدام طريقة الفروق المحددة و اعداد خوارزمية لحساب حركة تلك السوائل العضوية، الماء خلال الطبقة المشبعة من التربة. في الواقع يتكون النظام من ثلاثة اطوار من السوائل (ماء، سوائل عضوية اقل من الماء (DNAPL) والهواء) لكن عند اشتقاق النموذج الرياضي تم معاملة الهواء كطور غير متحرك مع ثبوت ضغط الهواء عند الضغط الجوي. ان المعادلات التي تصف حركة الماء و السوائل العضوية وضعت بدلالة عمود الضغط لتلك السوائل. أن معادلات الفروقات المحددة حلت

(fully implicitly) وباستخدام طريقة (Newton-Raphson) مع (Taylor series) لمعالجة المعادلات اللاخطية. تمت عملية اختبار كفاءة النموذج الحالي من خلال مقارنة نتائجه مع نتائج النموذج المقدم من قبل Kueper and Frind (1991b) النتائج لجميع الاختبارات تشير إلى ان وجود حاجز (Len) يسيطر على الحركة العمودية (DNAPL<sub>s</sub>) خلال الوسط غير المتجانس .

## INTRODUCTION

Groundwater is one of the most widespread sources of water, and because of its extensive use, ground water contamination has become a major environmental concern. The great majority of groundwater contaminants are released either from leaking hazardous waste landfills and hazardous waste ponds, or from spills and leaks during the storage and transportation of Non-Aqueous Phase Liquids (NAPL<sub>s</sub>). The reason why NAPL<sub>s</sub> entering soil and ground water system consider serious because of the major environmental health and safety problems associated with hydrocarbon discharge to the subsurface environment (Hall and Quam, 1976). Hydrocarbon products are typically multi-component organic mixtures composed of chemicals with varying degree of water solubility. These components are carcinogenic and some at least have some diverse health effects (Haskell, 1997; Ali, 2002) (Saleem, 2005).

As the oil migrates, the quantity of mobile oil decreases due to the residual oil left behind. If the amount of oil spilled is small, all of the mobile oil will become exhausted and the oil will percolate no further. However, if the amount of oil spilled is large, mobile oil will reach the water table. When DNAPL such as Trichloroethylene (TCE) infiltrates into the soil in large amounts, gravity causes it to sink into the groundwater aquifer and remain at the bottom for extended periods of time (Kim and Corapcioglu, 2003).

Underground containment barriers are an important method of limiting and/or eliminating the movement of contaminants through the subsurface. Barriers are currently used for the containment of contaminated waste, as an interim step while final remediation alternatives are developed (or decided). The purpose and function of the containment system must be determined prior to design and construction of the barrier. Site characterization is an essential part of choosing an appropriate barrier (Rumer and Mitchell, 1996). The plume of NAPLs will migrate vertically downward under force of gravity until it reach low permeability layer. Then, it accumulates and migrates laterally. There are many subsurface barrier technologies commercially available and others in various stages of development such as: - (Slurry walls, Sheet pile walls, Frozen barriers ...etc) (Pearlman, 1999).

There is a significant progress in multi-phase flow modeling during the last two decades in groundwater. Multi-phase flow and transport model was presented by Abriola and Pinder (1985a). The one-dimensional, finite-difference model included an organic phase composed of one volatile and one nonvolatile organic component. Al-Dulaimi (2006) studied the infiltration and redistribution of Light Non-Aqueous Liquid for the state of three fluid phases (water, oil and air) in the unsaturated-saturated zone of the soil.

Migration of NAPL<sub>s</sub> can be controlled by barrier systems. Starting in the late 1950s, gelling liquids were used successfully in grouting by controlling the injection



operation. Particulate grouts generally cannot be injected into media finer than medium sand. In finer grain-size material, gelling liquids must be used (May et al. 1986). As noted by Karol (1990), gelling liquids have a greater radius of influence than particulate grouts due to their initial low viscosity before gelatin. Rumer and Ryan(1995) reported that while several techniques have been demonstrated as the pilot scale and others are currently under development, horizontal barrier construction has not been developed to the extent of the vertical barriers. Newman (1995) barrier-material Zeolites treated with the Surfactant Hexa Decyl Tri Methyl Ammonium (HDTMA). HDTMA effectively traps many types of organic and inorganic contaminants in soil, while allowing water to pass through the barrier as cited by (Basri, 2001). Wipfler (2003) focused on the effect of an inclined soil layer with respect to the water table. There is a wide variety of possible barrier systems for sanitary landfills of Municipal Solid Waste (MSW) (Rowe, 2005).

The present study is aimed to develop a multi-phase, two-dimensional, finite-difference numerical simulator which tracks the percentage of oil saturation as well as the lateral and vertical position of the oil plume in the subsurface, resulting from oil spillage, in the presence of clay minerals lens as a barrier at the specified times with different types of boundary conditions.

**METHODS**

The basis of the mathematical description of the multi-phase fluid flow in porous media is the mass conservation laws. In the present study, the pressure gradient in gas phase will be assumed negligible so that the gas pressure remains effectively constant at atmosphere (Faust et al., 1989). The mass balance equation for each of the fluid phase in Cartesian coordinates can be written as (Bear, 1972):-

$$-\frac{\partial}{\partial x_i}(\rho_f \cdot q_f) \mp Q_f = \frac{\partial}{\partial t}(\phi \cdot \rho_f \cdot S_f) \dots\dots\dots(1)$$

Darcy’s Law describes the relation between the flux and the individual phase pressure. The general multi-phase Darcy’s Law is given by:-

$$q_f = -\frac{k \cdot K_{rf}}{\mu_f} \left( \frac{\partial P_f}{\partial x_i} + \rho_f \cdot g \cdot \frac{\partial z}{\partial x_i} \right) \dots\dots\dots(2)$$

The relative permeability (Kr) is a non-linear function of saturation. It ranges in value from 0 when the fluid is not present, to 1 when the fluid is present. Darcy’s law can be written equivalently in the form of the pressure head as below:

$$q_f = -K_f \left( \frac{\partial h_f}{\partial x_i} + \frac{\rho_f}{\rho_w} \cdot \frac{\partial z_i}{\partial x_i} \right) \dots\dots\dots(3)$$

By substituting Eq.(3) into Eq.(1), assume that the fluid and the porous medium are incompressible, and ignore the source-sink term, the resulting equation can be represented by:-

$$\frac{\partial}{\partial x_i} \left[ K_f \left( \frac{\partial h_f}{\partial x_i} + \frac{\rho_f}{\rho_w} \frac{\partial z}{\partial x_i} \right) \right] = \phi \frac{\partial S_f}{\partial t} \dots\dots\dots(4)$$

**Two-Dimensional Numerical Solution**

The previously derived mass balance equation (Eq.4) will be re-written as two equations in two-dimension, one for water phase and other for oil phase and expressed in terms of the phase pressure head as below:-

$$\frac{\partial}{\partial Z} \left[ K_w \left( \frac{\partial h_w}{\partial Z} + 1 \right) \right] + \frac{\partial}{\partial X} \left[ K_w \frac{\partial h_w}{\partial X} \right] = C_w \frac{\partial h_w}{\partial t} \dots\dots\dots(5)$$

$$\frac{\partial}{\partial Z} \left[ K_o \left( \frac{\partial h_o}{\partial Z} + \rho_{ro} \right) \right] + \frac{\partial}{\partial X} \left[ K_o \frac{\partial h_o}{\partial X} \right] = C_o \frac{\partial h_o}{\partial t} \dots\dots\dots(6)$$

where  $K_w = K_{ws} K_{rw}$  and  $K_o = K_{os} K_{ro} = \frac{K_{ws} K_{ro}}{\mu_{ro}}$ ; and  $C$  is the specific fluid capacity, It is defined by  $C_w = \phi \frac{\partial S_w}{\partial h_w}$  &  $C_o = \phi \frac{\partial S_o}{\partial h_o}$ .

The solution techniques used here consist of a finite-difference approximation (implicit method), the Newton-Raphson with a Taylor series expansion to treat the nonlinearities, and direct matrix solution (Gauss-Elimination method). These techniques result in the following equations:-

$$a_{fi,j}^k \delta_{fi-1,j}^{k+1} + b_{fi,j}^k \delta_{fi,j-1}^{k+1} + c_{fi,j}^k \delta_{fi,j}^{k+1} + d_{fi,j}^k \delta_{fi+1,j}^{k+1} + e_{fi,j}^k \delta_{fi,j+1}^{k+1} = -r_{fi,j}^k \dots\dots\dots(7)$$

where

$$a_{fi,j}^k = \left[ -R1 \left( K_{fi-1,j}^k + h_{fi-1,j}^k \frac{\partial K_{fi-1,j}^k}{\partial h_{fi-1,j}^k} \right) - R2 \frac{\partial K_{fi-1,j}^k}{\partial h_{fi-1,j}^k} \right]$$

$$b_{fi,j}^k = \left[ -R3 \left( K_{fi,j-1}^k + h_{fi,j-1}^k \frac{\partial K_{fi,j-1}^k}{\partial h_{fi,j-1}^k} \right) \right]$$

$$c_{fi,j}^k = \left[ C_{fi,j}^k + (h_{fi,j}^k - h_{fi,j}^n) \frac{\partial C_{fi,j}^k}{\partial h_{fi,j}^k} + R1 K_{fi-1,j}^k + R11 \left( K_{fi,j}^k + h_{fi,j}^k \frac{\partial K_{fi,j}^k}{\partial h_{fi,j}^k} \right) + R2 \frac{\partial K_{fi,j}^k}{\partial h_{fi,j}^k} \right. \\ \left. + R3 K_{fi,j-1}^k + R33 \left( K_{fi,j}^k + h_{fi,j}^k \frac{\partial K_{fi,j}^k}{\partial h_{fi,j}^k} \right) \right]$$

$$d_{fi,j}^k = -R11 K_{fi,j}^k$$

$$e_{fi,j}^k = -R33 K_{fi,j}^k$$

$$C_{fi,j}^k (h_{fi,j}^k - h_{fi,j}^n) - R1 K_{fi-1,j}^k h_{fi-1,j}^k + R1 K_{fi-1,j}^k h_{fi,j}^k + R11 K_{fi,j}^k h_{fi,j}^k - R11 K_{fi,j}^k h_{fi+1,j}^k - R2 K_{fi-1,j}^k \\ + R2 K_{fi,j}^k - R3 K_{fi,j-1}^k h_{fi,j-1}^k + R3 K_{fi,j-1}^k h_{fi,j}^k + R33 K_{fi,j}^k h_{fi,j}^k - R33 K_{fi,j}^k h_{fi,j+1}^k = r_{fi,j}^k$$

$$R1 = \frac{\Delta t}{\Delta Z_i (Z_{i-1} - Z_i)} \quad , \quad R11 = \frac{\Delta t}{\Delta Z_i (Z_i - Z_{i+1})} \quad , \quad R2 = \frac{\Delta t}{\Delta Z_i} \quad , \quad R3 = \frac{\Delta t}{\Delta X_j (X_{j-1} - X_j)}$$

$$\& \quad R33 = \frac{\Delta t}{\Delta X_j (X_j - X_{j+1})}$$

**Fig.1** (a) shows soil cross section for unsaturated-saturated zone and Fig.1 (b) shows the discretized domain in X-Z plane with time.

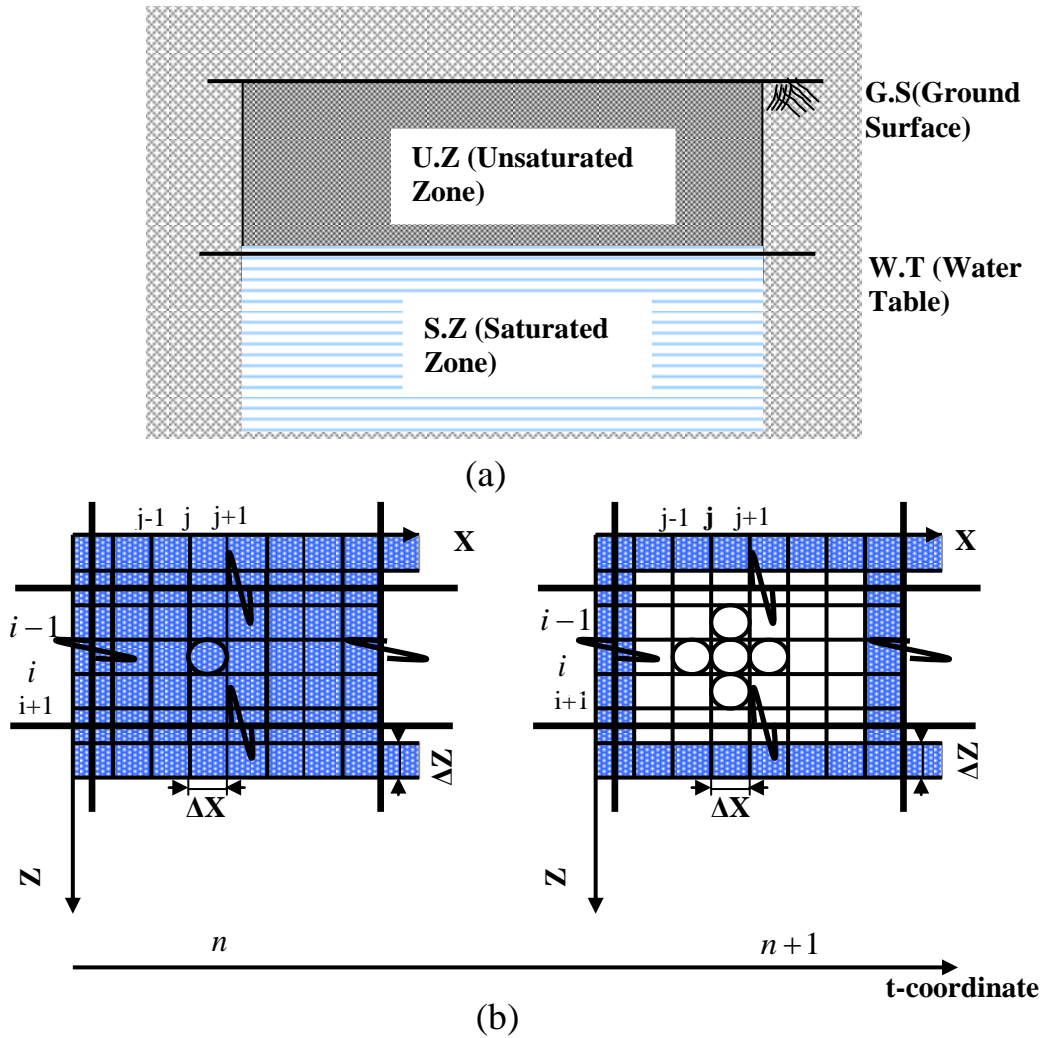


**Fig.1** : (a) The common situation to the virtual solution cross section, (b) Image to the solution domain.

The coefficients in Eq.(7)  $a, b, c, d$  and  $e$  are associated with  $\delta_{fi-1,j}^{k+1}, \delta_{fi,j-1}^{k+1}, \delta_{fi,j}^{k+1}, \delta_{fi+1,j}^{k+1}$  &  $\delta_{fi,j+1}^{k+1}$  respectively, and in general it is formed as:-

$$A^k \delta^{k+1} = -r^k \tag{8}$$

Where  $A = (a_{i',j'})$  is the coefficient matrix for the linearized system. The collection of equations for each solution node leads to have global diagonal coefficient matrix (its bandwidth equal to  $(2 * noc + 1)$ ). This matrix is solved for  $\delta$  and then the algorithm enters the next iteration with new values of  $h_f$  is evaluated as follows:-

$$h_{fi,j}^{k+1} = h_{fi,j}^k + \omega_f^{k+1} \delta_{fi,j}^{k+1} \tag{9}$$

With highly nonlinear flow problems, the updating method introduced by Cooley (1983) which introduces an optimal relaxation scheme, which accounts for the

maximum convergence error for entire mesh, is used in the present study in conjunction with Newton–Raphson scheme. The convergence criterion used here for a given phase  $f$  ( $=o,w$ ) is as follows:-

$$\frac{\max |\delta_{fi}^{k+1}|}{\max |h_{fi}^k + \delta_{fi}^{k+1}|} \leq \varepsilon \quad \dots\dots\dots(10)$$

A typical convergence criterion for pressure head is 0.001 or less. A computer program written in MATLAB (version 6.5) was developed to implement the model described above. Inherent in any subsurface modeling algorithms are assumptions and limitations. The major assumptions include:-

- The pressure in the air phase is constant and equal to atmospheric pressure.
- Both water and NAPL viscosities and densities are pressure independent.
- Relative permeability of water is a function of water saturation.
- Relative permeability of NAPL is a function of air and water saturations.
- Capillary pressure is a function of water saturation.
- Air saturation is a function of NAPL pressure.
- Darcy’s equation for multiphase flow is valid
- Intrinsic permeability is a function of space and there is no inter-phase mass transfer ( i.e ; the NAPL is truly immiscible in water).

The major limitations include:-

- Fractured systems are not treated; transport of dissolved NAPL is not treated
- The volatilization is not considered.

**Constitutive Relationships**

Modeling of two-phase flow in porous media requires specification of functional relationships between capillary pressure-saturation ( $P_c - S$ ) and relative permeability-saturation ( $K_r - S$ ).The fluid saturation is a function of the difference between the pressures of the two fluids in the porous medium. This pressure difference is called the capillary pressure ( $P_{ow} = P_o - P_w$ ), or capillary pressure head ( $h_{ow} = h_o - h_w$ ).For two-phase system, the capillary pressure-saturation ( $P_c - S$ ) relations are typically determined experimentally and fitted with some empirical mathematical functions either a Brooks and Corey as cited by (Kueper and Frind, 1991b) or (Van Genuchten, 1980). The capillary pressure-saturation relationship ( $P_c - S$ ) developed by Brooks and Corey (1964) is adopted in the present study. These relations are:-

$$S_e = \left( \frac{h_{ow}}{h_d} \right)^{-\lambda} \quad h_{ow} \geq h_d \quad \dots\dots\dots(11)$$

$$\bar{S}_t = \left( \frac{h_{ao}}{h_d} \right)^{-\lambda} \quad \dots\dots\dots(12)$$

$$K_{rw} = S_e^{\left[ \frac{(2+3\lambda)}{\lambda} \right]} \quad \dots\dots\dots(13)$$

$$K_{rnw} = (1 - S_e)^2 \left( 1 - S_e^{\left[ \frac{(2+3\lambda)}{\lambda} \right]} \right) \quad \dots\dots\dots(14)$$

## EFFECT OF CAPILLARY PROPERTIES ON FLUID BEHAVIOR ABOVE A SINGLE LENS

A theoretical work presented by Kueper and Frind (1991b) was used as verification to the study of influence of porous media properties on the spreading of a non-wetting fluid above a single lens of low relative permeability. Numerical simulations were carried out within the solution domain illustrated in Fig.2. This system consists of a 200 cm-wide by 35 cm-high porous medium containing a single 5 cm-thick lens of low relative permeability material, the top of which is situated 15 cm below the upper boundary. The left- and right-hand side boundaries are subjected to a constant wetting phase pressure representative of hydrostatic conditions and are maintained fully saturated by water at all times. The top and bottom boundaries are set impermeable to each of the wetting and non-wetting phases, except for middle 4 cm of the top boundary which acts as the source area for the entry of non-wetting fluid under a small water equivalent TCE head of 29.9 cm to simulate an TCE spill. This source area is characterized by a constant wetting phase pressure and a constant distribution of fluid distribution.

The outlined solution domain with its prescribed boundary conditions is discretized into 800 finite-difference cells with constant nodal spacing of 5 cm in the vertical direction and 2 cm in horizontal direction. The initial condition in the cell is a hydrostatic distribution of wetting phase pressure, with the water table coinciding with the top of the solution domain and 100% saturation of the wetting phase throughout.

Variable time step sizes were used to solve this problem. Initially, when the infiltrating pressure front is steep and, consequently, the nonlinearities are strong, the small time step must be chosen. In this case, the initial time step size was 0.000001 hours. As time passes the infiltrating front smoothes and the nonlinearities weaken. This can be seen as the Newton-Raphson iteration scheme requires less iteration to converge as time passes. As the amount of iterations decreases, the time step size is increased. The final time step size was 0.1 hours for this simulation.

The simulations illustrate the effect of permeability of the 5 cm-thick lens on the spreading of a non-wetting phase infiltrating vertically downward from the source area. The non-wetting phase was assigned density of  $1400 \text{ kg/m}^3$  and a viscosity of  $0.57 \times 10^{-3} \text{ Pa.s}$ . The wetting phase was assigned a density of  $1000 \text{ kg/m}^3$  and viscosity of  $1.0 \times 10^{-3} \text{ Pa.s}$ . The source boundary condition was specified with a wetting phase pressure of 0.00 Pa and wetting phase saturation of 0.50. The fluid properties are characteristic of Tetrachlorethylene (TCE) a commonly used industrial solvent.

The host material of the solution was assigned permeability of  $K_f = 24.7 \text{ cm/hr}$  ( $k = 7.0 \times 10^{-12} \text{ m}^2$ ), while lens was assigned a range of permeabilities slightly lower than that of the host material. The parameters of porous media used in the present simulation are given in Table (1).

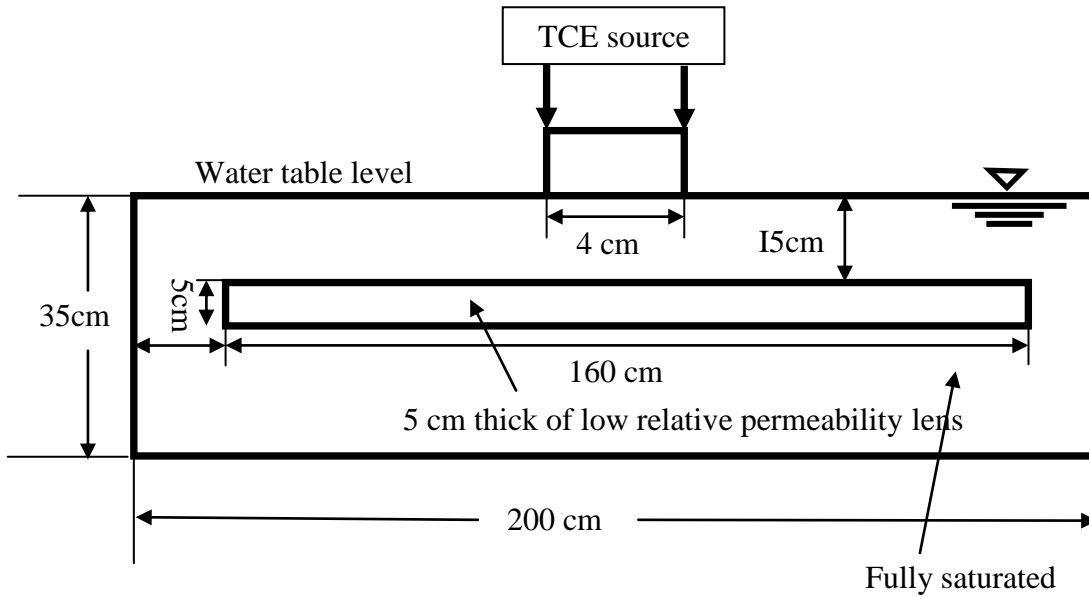


**Fig.2: Solution domain for single lens simulations (Kueper and Frind, 1991b).**

**Table1: Porous media properties used for simulation (Kueper and Frind, 1991b).**

parameters	values
Host permeability , cm/hr ( $K_{swH}$ )	24.7
Lens permeability, cm/hr ( $K_{swL}$ )	17.6
Host displacement pressure. cm ( $P_{dh}$ )	22.6
Lens displacement pressure .cm ( $P_{dl}$ )	28.6
Residual wetting phase % ( $S_r$ )	7.8
Pore size distribution index ( $\lambda$ )	2.48
Porosity ( $\phi$ )	0.34

## RESULTS AND DISCUSSION

The theoretical results of case study are compared with results of Kueper and Frind (1991b) as shown in Fig.3, Fig.4. There is a satisfactory agreement between the present results and those of Kueper and Frind (1991b). Fig.5 illustrates the distribution of non-wetting fluid in the solution domain for the case where the low relative permeability lens was assigned a permeability of  $K_f = 17.6$  cm/hr ( $k = 5.0 \times 10^{-12}$  m<sup>2</sup>) for times (0.57 hour, 1.13 hour, 1.99 hour and 4.59 hour) as calculated by the present model. In these figures, the darker shades indicate higher TCE content and the lighters shades lower TCE contents. According to these figures, non-wetting fluid encountered the lens; it would pool and spread laterally, allowing for a build up of saturation immediately above the lens. Once this saturation brings about a capillary pressure in excess of the displacement pressure of the lens,



penetration takes place. Lateral spreading continues beyond this point of penetration, since the lower permeability lens cannot transmit non-wetting fluid at a rate equal to the higher permeability host material.

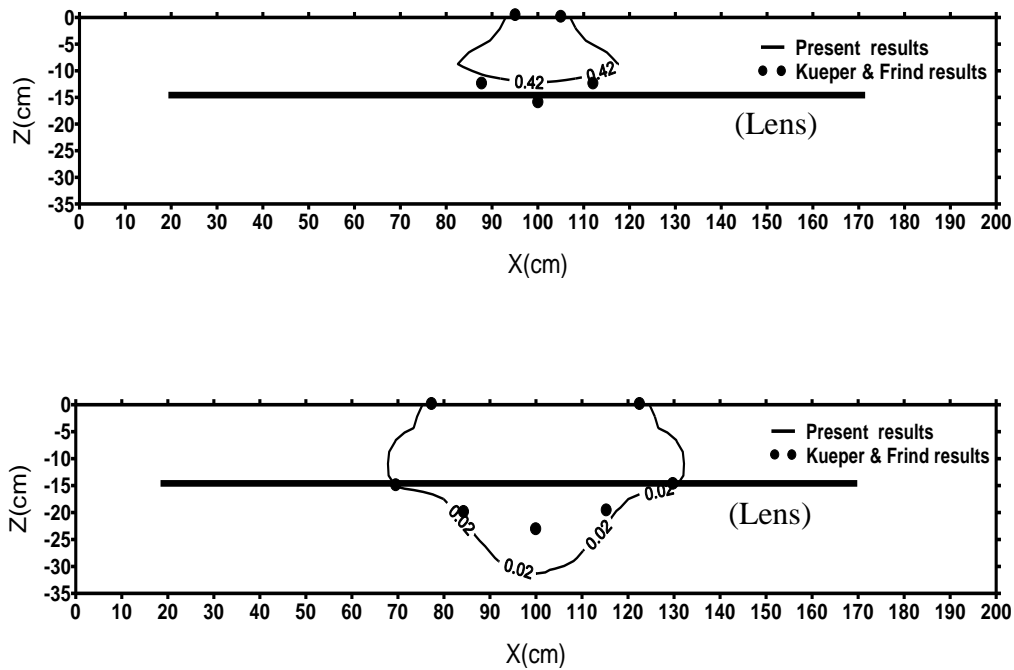


**Fig.3: DNAPL plume location during infiltration after 1.99 hour when (a) DNAPL Saturation=0.42 & (b) DNAPL saturation=0.02.**

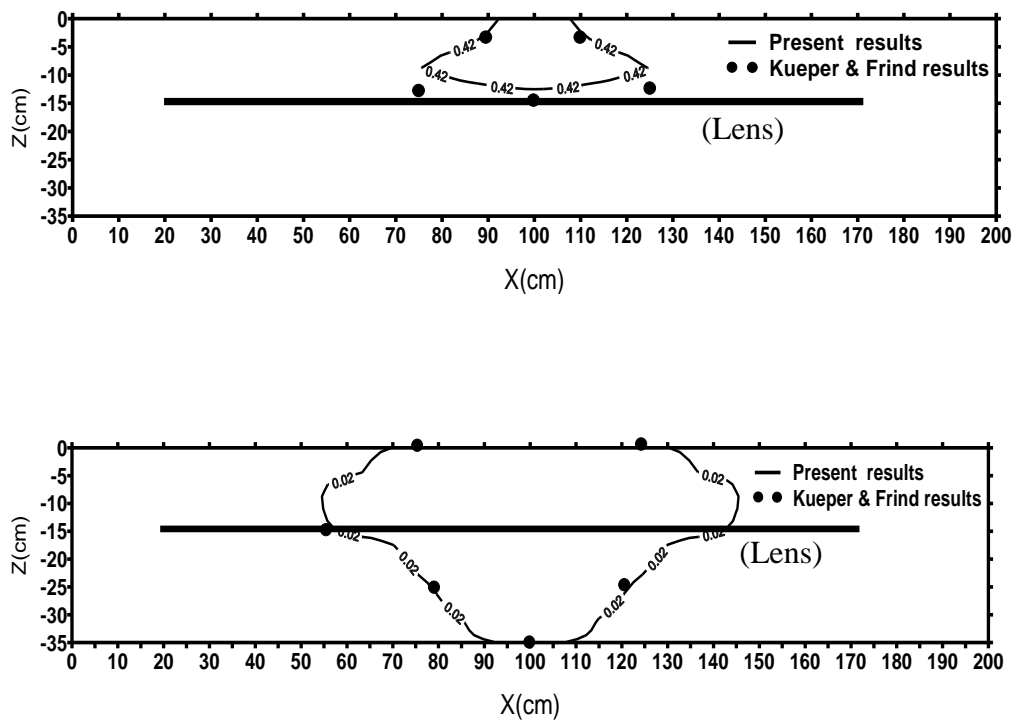


**Fig.4: DNAPL plume location during infiltration after 4.59 hour when**

(a) DNAPL Saturation=0.42 & (b) DNAPL saturation=0.02.

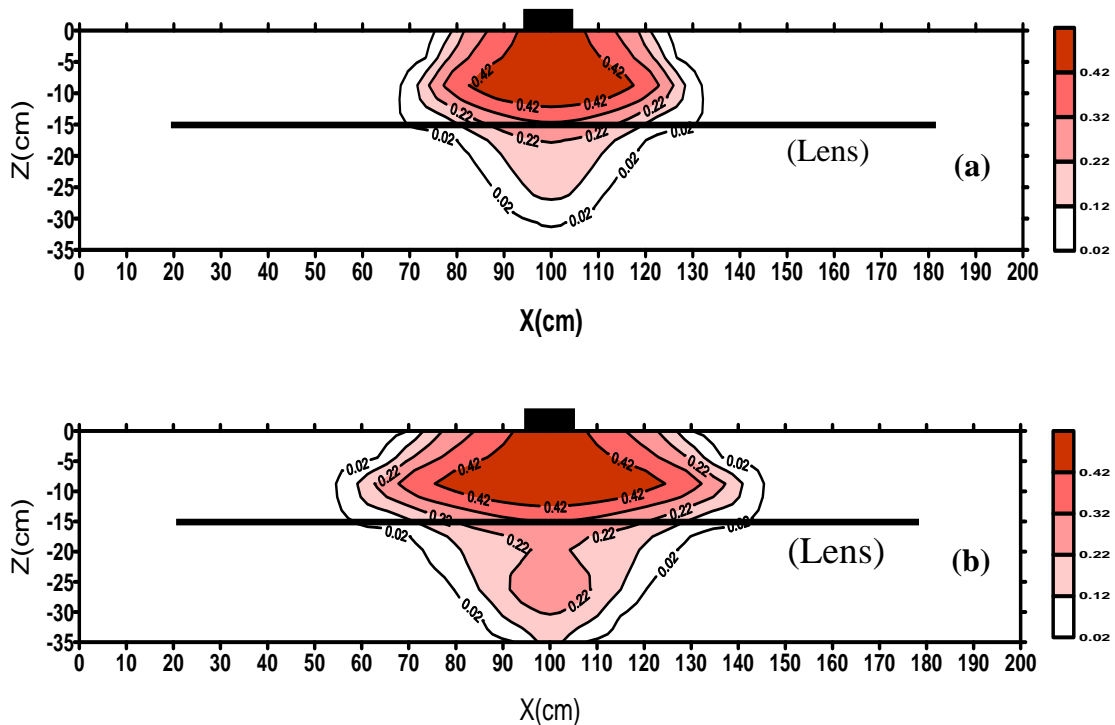


Fig.5: DNAPL saturation after (a) 1.99 hour and (b) 4.95 hour.

## CONCLUSIONS

The following conclusions can be deduced:-

- The numerical solution employed in this study based on the potential form of the governing equations with techniques consisted of Implicit Finite Difference, Newton-Raphson and Gauss-Elimination schemes showed to be an efficient procedure in solving problems of two-dimensional water and NAPL<sub>s</sub> flow through the unsaturated and/or saturated zone of three fluid phases system in the presence of low relative permeability lens.
- During infiltration of DNAPL, the maximum saturation occurred below the source and when it advanced the saturation will decrease.
- Observations of (DNAPL) plume migration through heterogeneous porous media, upon encounter with a low relative permeability lens, the non-wetting fluid must build up the required saturation to generate the necessary capillary pressure facilitating entry into the lens. This build up of saturation give rise to lateral pressure gradients, promoting lateral spreading of non-wetting fluid above the low relative permeability lens. Once the lens has been penetrated, lateral spreading continues because of inability of the lens to transmit fluid at rate equal to that of the higher-permeability material immediately above the lens.

**REFERENCES**

- Abriola, L. M., and G. F. Pinder, "A multi-phase approach to the modeling of porous media contamination by organic compounds: 1. Equation development". *Water Resources Research*, 21(1), 11-18, 1985a.
- Al-Dulaimi, A. A. H., "Numerical Modeling of Light Non-Aqueous Phase Liquid Spill Transport in an Unsaturated-Saturated Zone of the Soil". Ph.D. Thesis, Baghdad University, 2006.
- Basri, M. H., "Two New Methods for Optimal Design of Subsurface Barrier to Control Seawater Intrusion". Ph.D. Thesis, Manitoba University, 2001.
- Bear, J., "Dynamics of fluids in porous media". Elsevier, New York, 1972.
- Cooley, R. L., "Some new procedures for numerical solution of variably saturated flow problems". *Water Resources Research*, 19(5), 1271-1285, 1983.
- Durmusoglu, E., and M. Y. Corapcioglu, "Experimental study of horizontal barrier formation by Collidal silica". *Journal of Environmental Engineering*, 126(9), 833-841, September, 2000.
- Faust, C. R., J. H. Guswa, and J. W. Mercer, "Simulation of three-dimensional flow of immiscible fluids within and below the unsaturated zone". *Water Resources Research*, 25(12), 2449-2464, 1989.
- Hall, P. L., and H. Quam, "Countermeasures to control oil spills in western Canada". *Groundwater*, 14, 1976.
- Karol, R. H., "Chemical grouting". 2nd Ed., Marcel Dekker, New York, 1990.
- Kim, J., and M. Y. Corapcioglu, "Modeling dissolution and volatilization of LNAPL sources migrating on the groundwater table". *J. of Contaminant Hydrology*, 65, 137-158, 2003.
- Kueper, B., and E. Frind, "Two-phase flow in heterogeneous porous media: 2. Model application". *Water Resources Research*, 27(6), 1059-1070, 1991b.
- May, J. H., R. J. Larson, P. G. Malone, J. A. Boa, and D. L. Bean, "Grouting techniques in bottom sealing of hazardous waste sites". Rep. EPA/600/S2-86/020, U.S. Environmental Protection Agency, Cincinnati, 1986.
- Newman, A., "Subsurface barrier trapped diverse contaminants, let water through". *Environmental / Science & Technology*, 29(8), 1995.
- Pearlman, L., "Subsurface containment and monitoring system: Barriers and beyond". [www.epa.gov/tio/download/remed/Pearlman.pdf](http://www.epa.gov/tio/download/remed/Pearlman.pdf), 1-61, 1999.
- Rowe, R. K., "Long-term performance of contaminant barrier system". [www.geoeng.ca/Directory/kerryPub/GeotechniqueRankine/Rowe.pdf](http://www.geoeng.ca/Directory/kerryPub/GeotechniqueRankine/Rowe.pdf), 55(9), 631-678, 2005.
- Rumer, R. R., and M. E. Ryan, "Barrier containment technologies for environmental remediation applications". Wiley, New York, 1995.

- Rumer, R. R., and J. K. Mitchell, "Assessment of barrier containment technologies a comprehensive treatment for environmental remedial application" Product of the
- International Containment Technology Workshop. National Technical Information Service, PB96-180583, 1996.
- Saleem, M., "Assessment of the Relation between the Spilled LNAPL Volume and its Thickness in Monitoring Well Considering the Water Table Fluctuation History". Ph.D. Thesis, King fahd University of Petroleum and Minerals, 2005.
- Van Genuchten, M., "A closed-form equation for predicting the hydraulic conductivity of unsaturated soils". Soil Sci. Soc. Am. J., 44, 892-898, 1980.
- Wipfler, E. L., "Effects of capillarity and heterogeneity on flow of organic liquid in soil". Ph.D Thesis, Wageningen University, Wageningen, library.wur.nl/wda/ dissertations/dis3384.pdf, 2003.

## SYMBOLS

$A$	Coefficient matrix	[————]
$C_w$	Specific water capacity	[————]
$C_o$	Specific oil capacity	[————]
$g$	Acceleration due to gravity	[m/s <sup>2</sup> ]
$h_f$	Fluid pressure head	[m]
$h_a$	Air pressure head	[m]
$h_{ao}$	Air-oil capillary pressure head	[m]
$h_o$	Oil pressure head	[m]
$h_{ow}$	Oil-water capillary pressure head	[m]
$h_w$	Water pressure head	[m]
$h_d$	Displacement pressure head	[m]
$i, j$	Grid identification in X,Z coordinates respectively.	[————]
$K_w$	Water Hydraulic conductivity	[m/s]
$K_o$	Oil Hydraulic conductivity	[m/s]
$K_f$	Hydraulic conductivity of phase $f$	[m/s]
$K_{fs}$	The conductivity when the medium is saturated with fluid $f$	[m/s]
$K_r$	Relative hydraulic conductivity	[————]
$K_{ro}$	Relative hydraulic conductivity of oil	[————]
$K_{rw}$	Relative hydraulic conductivity of water	[————]
$k$	The intrinsic permeability tensor of the medium in Eq. (2)	[————]
$k$	Iteration index	[————]
$K_{rf}$	Relative permeability of the phase $f$	[————]



$n$	Time step identification (if it is superscript)	[—]
$noc$	The number of columns	[—]
$non$	The $n^{\text{th}}$ grid identification	[—]
$nor$	The number of rows	[—]
$\lambda$	Pore size distribution index	[—]
$P_f$	Fluid pressure of phase $f$	[kg/m <sup>2</sup> ]
$P_c$	Capillary pressure of phase $f$	[kg/m <sup>2</sup> ]
$P_w$	Pressure of water phase	[kg/m <sup>2</sup> ]
$P_o$	Pressure of oil phase	[kg/m <sup>2</sup> ]
$Q_f$	Source or sink of phase $f$	[kg/m <sup>3</sup> s]
$q$	Volumetric flux (or Darcy's flux)	[m/s]
$r$	The residual due to approximation	[—]
$S$	Degree of saturation	%
$S_f$	Degree of fluid saturation	%
$S_a$	Degree of air saturation	%
$S_o$	Degree of oil saturation	%
$S_t$	Degree of total liquid saturation	%
$\bar{S}_t$	Degree of effective total liquid saturation	%
$S_e$	Degree of effective water saturation	%
$t$	Time coordinate	[s]
$X, Z$	Cartesian coordinates	[m]

### Greek symbols

$\delta$	The difference between the approximation and exact solution in fluid pressure head	[m]
$\varepsilon$	Convergence tolerance	[m]
$\mu_f$	Dynamic viscosity of fluid $f$	[kg/m s]
$\mu_{ro}$	Ratio of oil to water viscosity	[—]
$\rho_f$	Density of phase $f$	[kg/m <sup>3</sup> ]
$\rho_{ro}$	Ratio of oil to water density	[—]
$\rho_w$	Density of water at standard temperature and pressure	[kg/m <sup>3</sup> ]
$\phi$	Porosity of the medium	[m <sup>3</sup> /m <sup>3</sup> ]
$\omega$	Damping parameter	[—]
$\Delta t$	Time step size	[s]
$\Delta X$	Horizontal increment in X-direction	[m]
$\Delta Z$	Vertical increment in Z-direction	[m]